

Critical Behavior in Anchoring Transitions of Nematic Liquid Crystals

J. Bechhoefer,^(a) J-L. Duvail, L. Masson, B. Jérôme, R. M. Hornreich,^(b) and P. Pieranski
Laboratoire de Physique des Solides, Université de Paris-Sud, Bâtiment 510, 91405 Orsay CEDEX, France
 (Received 8 September 1989)

The adsorption of water onto a crystal surface can result in a first-order transition in the orientation of the director of a nematic liquid crystal spread on top of the surface. Here, we show that coadsorption of two or three chemicals can lead to a phase diagram having first-order transition boundaries, critical lines, and critical points. A simple Landau theory accounts for most of the phenomena we observe. This experiment gives the first direct optical visualization of a two-dimensional system near its critical point.

PACS numbers: 61.30.Eb

Over seventy years ago, Mauguin¹ and Grandjean² discovered that a crystal substrate can orient, or "anchor," a nematic liquid-crystal layer spread on top of it. Because of the anisotropy of the crystal surface, the energy of liquid-crystal molecules depends on their orientation. Recently, we showed that the anchoring direction can change discontinuously as the amount of water vapor adsorbed onto the crystal surface is changed.³⁻⁵ This jump is a first-order phase transition and has been dubbed the "anchoring transition."

In this Letter, we consider the effects of coadsorbing *two or three* chemicals onto the interface and show that the resulting anchoring transitions may have first-order transition lines and critical points. The latter can either terminate a first-order transition line or form a second-order transition line together with a critical end point. A simple Landau theory that takes into account the symmetry of the nematic phase and of the substrate yields a phase diagram that agrees qualitatively with our observations.

The transitions we study are two dimensional in that the liquid-crystal molecules *on the substrate surface* change their orientation. The molecules in the bulk simply follow the orientation of those on the interface, for their top surface is unconstrained. (Although the molecules at the free surface lie at an angle to that surface, the azimuthal projection of this angle is not fixed.) We can thus see changes in the orientation of a single molecular layer. Using this method, we have obtained the first direct optical visualization of a two-dimensional system near its critical point.

The liquid crystal used was the commercially prepared blend E9.⁶ We also obtained essentially the same results using the pure liquid crystal 50CB,⁶ which is a component of E9. Since E9 is nematic at room temperature, it was easier to work with than 50CB. In both cases, the transitions were reversible and repeatable.

We spread the liquid crystal in a layer a few microns thick on a substrate of muscovite mica. As the effects we study are controlled by adsorbed chemicals, it is important to use clean, freshly cleaved surfaces. The three chemicals that were adsorbed on and desorbed off the mica were water, methanol, and ethylene glycol.

The experimental apparatus is sketched in the inset in Fig. 1. The sample was observed through an optical microscope between crossed polarizers. A Soleil compensator balanced the mica's birefringence. The azimuthal orientation of the liquid crystal (LC) was determined by simultaneously rotating the crossed polarizers (P_1, P_2) until the image was extinguished. Measurements have an accuracy of $\pm 1^\circ$.

Most of the experiments were done using water and pure ethylene glycol. Their adsorption onto the surface was controlled by regulating their partial vapor pressures p , or, equivalently, their chemical potentials μ (for constant temperature). Thus, we control *intensive* variables, which are conjugate to densities of adsorbed molecules on the substrate.⁷ Note that, in general, there will be water and ethylene glycol adsorbed in the bulk nematic phase, as well as adsorbed onto the interface. However,

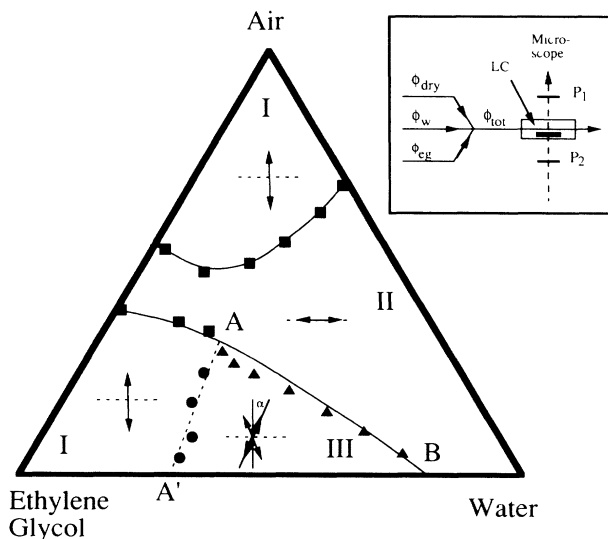


FIG. 1. Experimental ternary phase diagram. Solid lines (with squares and triangles) represent a first-order phase transition; the dashed line represents a continuous transition. At the I-II boundary, the orientation jumps 90° . At the II-III boundary, the orientation jumps 90° at A , decreasing smoothly to 60° at B . Inset: Sketch of the experimental apparatus.

a macroscopic thermodynamic description of anchoring transitions can be made without reference to the microscopic details of the system.

To control partial pressures, mass flow meters independently regulated flows of dry air⁸ (ϕ_{dry}), of saturated water vapor (ϕ_w), and of saturated ethylene-glycol vapor (ϕ_{eg}), so that their sum $\phi_{\text{tot}} = \phi_w + \phi_{\text{eg}} + \phi_{\text{dry}}$ was constant ($\phi_{\text{tot}} \cong 3 \text{ cm}^3/\text{sec}$). The observed stability of the flows was 0.1% of full scale. We could thus plot the ternary phase diagram as a triangle (see Fig. 1). A point in the corner of the diagram marked "water," for example, corresponds to $\phi_w = \phi_{\text{tot}}$, $\phi_{\text{eg}} = \phi_{\text{dry}} = 0$, so that $p_w = p_{\text{sat}}$. In experiments where methanol was the third adsorbed substance, a few percent was mixed with ethylene glycol. Because the amount of methanol in the ethylene glycol is fixed (and small), the resulting ternary diagram is actually a (low-angle) triangular slice in a four-component, tetrahedral phase diagram.

Figure 1 shows the measured anchoring phase diagram of E9 on muscovite mica using pure ethylene glycol. (Adding methanol to the ethylene glycol does not affect the topology of the diagram; however, region II shrinks toward the air-water edge of the phase diagram, and the line AA' becomes much longer.) The squares represent a first-order transition line of 90° discontinuity in the orientation of the liquid-crystal molecules (see Ref. 3 for a photograph of this transition). The triangles represent a line of first-order transitions, along which the orientation discontinuity varies from 90° at A to 60° at the edge of the phase diagram B . The circles represent a line of *continuous transitions* that starts at point A' at the water-ethylene-glycol edge of the ternary diagram and terminates at point A on the first-order transition line. All along the line AA' , orientation fluctuations are large.

The behavior of molecular orientations in region III

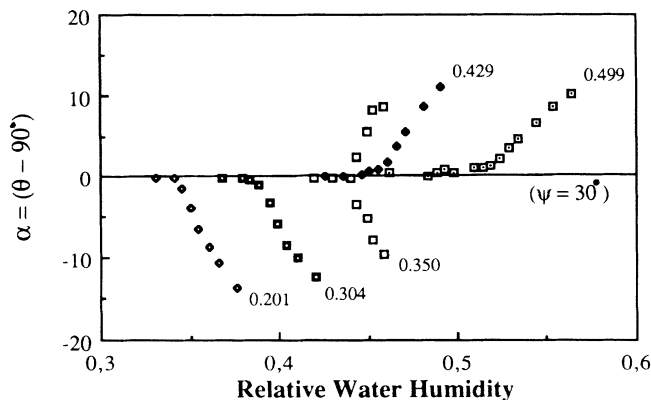


FIG. 2. Measurements of the orientation (α) of the molecules with respect to that of molecules in region I, as a function of water humidity. The different curves were measured along different points on the AA' line in Fig. 1. The values of ϕ_{dry} on the AA' line are indicated next to each curve. For $\phi_{\text{dry}} = 0.350$, two stable orientations were observed.

depends greatly on whether methanol is added to the ethylene glycol or not. For pure ethylene glycol, the orientation evolves continuously to $+30^\circ$ with respect to the optical axes as the line AA' is crossed. When methanol is added, the molecules turn $\pm 30^\circ$, depending on the value of ϕ_{dry} when crossing the line AA' . As shown in Fig. 2, for $\phi_{\text{dry}} < \phi_{\text{crit}} = 0.35$, the orientation evolves towards -30° ; for $\phi_{\text{dry}} > \phi_{\text{crit}}$, it evolves toward $+30^\circ$. When $\phi_{\text{dry}} = \phi_{\text{crit}}$ at the crossing, the anchoring bifurcates to bistable domains. We note, too, that whereas fluctuations could be observed anywhere along the line AA' , their amplitude (and spatial extent) was greatest at $\phi_{\text{dry}} = \phi_{\text{crit}}$.

Spatial variations caused the transition thresholds to vary slightly across the sample. This is illustrated in Fig. 3, where one domain is favored in the top part of each photograph and the other in the bottom part. In the middle, one sees critical fluctuations in Fig. 3(a) (on the line AA' , at $\phi_{\text{dry}} = \phi_{\text{crit}}$) and irregularly shaped domains in Fig. 3(b) (slightly to the right of the AA' line).

We can account for almost all of the above observations with a simple Landau theory for the surface potential of the liquid crystal. Since the molecules lie in the plane, the grand canonical potential may be expanded as

$$\Omega = \sum_{m=1}^{\infty} a_m \cos(m\theta + \delta_m), \quad (1)$$

where θ is the angle between the nematic director n and

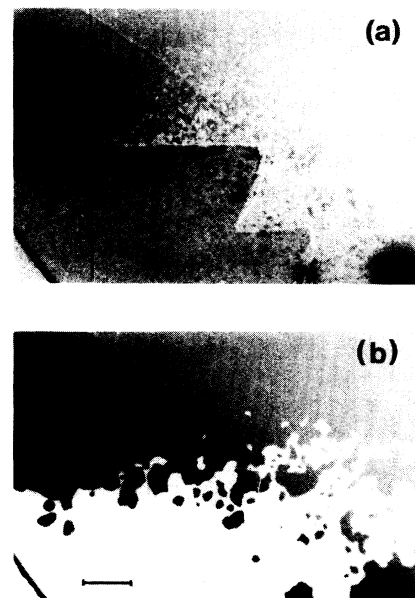


FIG. 3. Photographs of a region in the sample where the choice of the bifurcation branch at the I-III transition line (AA') is reversed; upper and lower branches are stable, respectively, in upper and lower halves of the photographs. (a) Critical fluctuations. (b) Domains are seen after the transition point is crossed. The bar is $200 \mu\text{m}$ long.

a fixed direction in the cleavage plane. Since nematics are invariant under $n \rightarrow -n$, only even values of m are allowed. The structure of a cleaved muscovite mica surface is complicated and has been described in detail elsewhere.⁴ The bulk crystal is composed of alternating AB layers and may be cleaved to expose either the A or B plane. Each A and B layer is itself composed of two slightly distorted honeycomb lattices displaced one from another. The direction of the displacement vector in B planes is rotated 120° with respect to that of A planes. The honeycomb structures have a distorted hexagonal, C_{3v} symmetry but each A or B layer has only a mirror, C_S symmetry because of the shifted sublayers. Thus, there are mirror planes (M_A and M_B) lying at $\pm 120^\circ$ from the optical axis of the crystal, the choice of sign depending on whether the surface is an A or B plane. By measuring angles relative to the mirror plane of the surface layer, we may set the phases (δ_m) in Eq. (1) equal to zero. Given the hexagonal symmetry, we expect the $m=2, 4,$ and 6 terms in Eq. (1) to be important. We then have

$$\Omega = -a \cos 2\theta + b \cos 4\theta - \cos 6\theta, \quad (2)$$

where the coefficients have been normalized with respect to $|a_3|$, renamed, and their signs chosen for later convenience. Here, the coefficients a and b are functions of the relative humidities (p/p_{sat}), or, equivalently, the chemical potentials μ_w and μ_{eg} of water and ethylene glycol. In work to be reported elsewhere, we show that a and b depend on temperatures only via $p_{\text{sat}}(T)$.⁹

Examining Ω and its derivatives, we obtain the theoretical phase diagram shown in Fig. 4. Like the experimental diagram in Fig. 1, there are three regions (I, II, and III), separated by transition lines. The discontinuity of the orientation between regions I and II is 90° ; between II and III, it varies from 90° at point A to 60° at point B . The dashed line AA' between I and III is a line of second-order anchoring transitions; the bifurcation is perfect for any point on this line.

In real samples, the bifurcation along the AA' line is perfect only for one point on the AA' line. Also, the difference in angle between regions I and II was not rigorously 90° but rather 86° to 88° . These effects can be modeled by adding a small anisotropy bias to Eq. (2). Since the $\theta \rightarrow \theta + \pi$ symmetry of the nematic is not broken, the lowest-order term will have the form $\epsilon \sin 2\theta$, where $\epsilon(x, t, \mu)$ is a slowly varying function of space, time, and chemical potentials. This, in fact, can model the variations described above. For example, upon expanding the grand canonical potential about $\theta = 90^\circ + \alpha$, we arrive at

$$\Omega = \Omega_0 + a^* \alpha^2 - b^* \alpha^4 - \epsilon^* \alpha. \quad (3)$$

Here, a^* and b^* are linear functions of a and b , and $\epsilon^* = 2\epsilon$. This is the well-known form of the mean-field free energy of an Ising model in the presence of an exter-

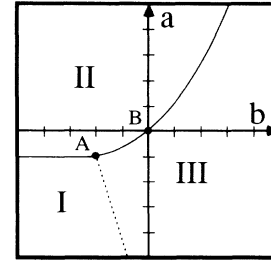


FIG. 4. Theoretical phase diagram, from Eq. (2). At the solid line separating regions I and II, the nematic orientation jumps 90° . The dashed line between regions I and III marks a second-order transition. Between regions II and III, the orientation jumps 90° at A and decreases smoothly to 60° at B .

nal field.¹⁰ The magnetization M is analogous to the angle α between the orientation of the molecules in region I and the domains in region III. The coefficient ϵ^* is then the field conjugate to the order parameter α . Because of this anisotropy, the diagram of Fig. 4 should be modified. Suppose that, for given x and t , there is a line $a = a(b)$, defined by $\epsilon^* = 0$, which crosses the line AA' at some point C . Then, strictly speaking, the second-order transition line AA' is suppressed except at the point C , at which there is a critical point terminating the first-order transition line defined by $\epsilon^* = 0$. In the magnetic analogy, the point C is the Curie point on a (T, H) diagram, and the first-order transition line is the line $H = 0$ for $T < T_C$. As a test of these ideas, we selected a large, defectless region in the sample, where critical fluctuations such as those shown in Fig. 3(a) occurred at one point C on the line AA' . We brought the sample into region I of the phase diagram and moved rapidly into region III on a path crossing the line AA' above the point C . Domains symmetrically oriented with respect to the mirror plane were initially nucleated but then the domains of one sign expanded at the expense of the others. Moving further down in region III, we reversed this expansion. In other words, a first-order line, ending at the critical point C , was crossed.

The anisotropy bias ϵ^* in Eq. (3) results from breaking the substrate symmetry of the substrate from C_S to C_1 . For muscovite mica, the mirror symmetry is broken once interactions with crystal layers beneath the mica surface are taken into account. For substrates with perfect C_S the whole second-order transition line would be observable, and we would be free from having to compensate for the anisotropy bias. The symmetry breaking could then be obtained, for example, by adsorbing chiral molecules or by mechanically stressing the sample in a suitable symmetry direction.

Although the anisotropy ϵ^* is permitted by symmetry, its variation with position, time, and chemical potentials is not understood. The problem is the same as that of explaining the variation of the other Fourier coefficients in Eq. (1) and is a limitation of any phenomenological

model. More physically, spatial variations can clearly be associated with optically visible surface defects. As for the temporal variations, an obvious source is surface contamination. Another possibility is surface reconstruction,¹¹ which would occur on longer time scales. But more important, we need to understand why the transitions take place. Our only clue is that the chemicals inducing the anchoring transition (water, alcohols, diols) form hydrogen bonds to the mica substrate. They thus adsorb to mica in preference to the liquid crystal, which is affected mainly by van der Waals forces. One sees that surface structure may be modified by adsorption, but the transition mechanism itself remains mysterious.

Beyond these unresolved problems concerning the microscopic mechanism of anchoring transitions, other more universal theoretical issues remain open. For example, how does the essentially semi-infinite character of the liquid-crystal layer affect the two-dimensional nature of the transition at the interface? For magnets, one knows¹² that surface critical behavior is modified by the presence of a semi-infinite bulk system. In addition, since the continuous anchoring transition is between ordered phases and therefore analogous to spin reorientation in magnetic systems, one also expects coupling to elastic degrees of freedom to affect the nature of the critical behavior.¹³ Measurements of critical exponents will be of great value in answering these questions.

We thank P. Pfeuty for useful discussions. This work was supported in part by NSF Grant No. INT-8808354, a Chateaubriand Fellowship, and by the Ministère de la Recherche et de la Technologie.

Note added.—After this work was completed, we learned that Guenoun, Perrot, and Beysens have observed directly critical fluctuations in a *three-dimensional* system.¹⁴

^(a)Current address: Laboratoire de Physique des Solides, Ecole Normale Supérieure de Lyon, 46 allée d'Italie, 69364 Lyon CEDEX 07, France.

^(b)Permanent address: Department of Electronics, Weizmann Institute of Science, 76100 Rehovot, Israel.

¹C. Mauguin, *Bull. Soc. Fr. Cryst.* **34**, 71 (1911).

²F. Grandjean, *Bull. Soc. Fr. Cryst.* **39**, 164 (1916).

³P. Pieranski and B. Jérôme, *Phys. Rev. A* **40**, 317 (1989).

⁴P. Pieranski, B. Jérôme, and M. Gabay, in *Proceedings of the Second International Conference on Optics of Liquid Crystals*, Torino, 1988 [*Mol. Cryst. Liq. Cryst.* (to be published)].

⁵P. Pieranski and B. Jérôme, in *Phase Transitions in Soft Condensed Matter*, edited by T. Riste, NATO Advanced Study Institutes Ser. B, Vol. 211 (Plenum, New York, 1989).

⁶British Drug House Chemicals, Ltd. (BDH), Poole, England. "E9" is a mixture of four different cyanobiphenyl and cyanoterphenyl nematogens, with the following composition: 15% 30CB, 38% 50CB, 38% 70CB, and 9% 5CT. "50CB" is an abbreviation of 4-*n*-pentyloxy-4'-cyanobiphenyl and is sold by BDH as "M15."

⁷R. Pandit, M. Schick, and M. Wortis, *Phys. Rev. B* **26**, 5112 (1982).

⁸Mass Flow Controller Model F-201, Bronkhorst High Tech B. V., Ruurlo, The Netherlands.

⁹J. Bechhoefer, B. Jérôme, and P. Pieranski, *Phys. Rev. A* **41**, 3187 (1990).

¹⁰See, for example, L. E. Reichl, *A Modern Course in Statistical Physics* (Univ. of Texas, Austin, 1980), Chap. 4, especially p. 110.

¹¹K. Müller and C. C. Chang, *Surf. Sci.* **14**, 39 (1969); D. Haneman, *Adv. Phys.* **31**, 165 (1982).

¹²H. W. Diehl, *J. Appl. Phys.* **53**, 7914 (1982).

¹³R. M. Hornreich and S. Shtrikman, *J. Phys. C* **9**, L683 (1976).

¹⁴P. Guenoun, F. Perrot, and D. Beysens, *Phys. Rev. Lett.* **63**, 1152 (1989).

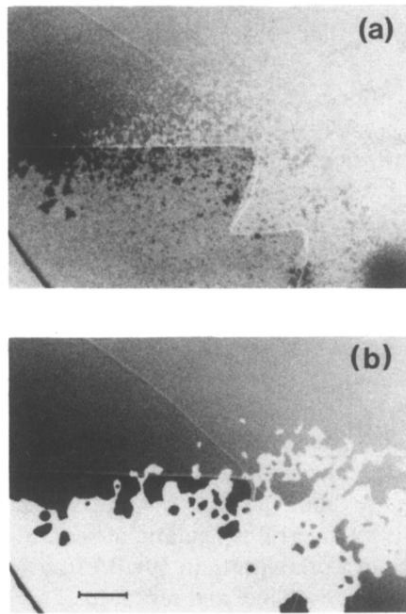


FIG. 3. Photographs of a region in the sample where the choice of the bifurcation branch at the I-III transition line (AA') is reversed; upper and lower branches are stable, respectively, in upper and lower halves of the photographs. (a) Critical fluctuations. (b) Domains are seen after the transition point is crossed. The bar is $200\ \mu\text{m}$ long.